A Saturated Light Correction Method for DMSP-OLS Nighttime Stable Light Data by Remote and Social Sensing Data

Xiaolei Huang, Kaifang Shi, Yuanzheng Cui, and Yuanqing Li

***Abstract*—The defense meteorological satellite program- operational line-scan system nighttime stable light (NTL) data have been widely used to evaluate the intensity of human activities. However, the sensor's defects lead to the saturation phenomenon, which greatly limits the reliability of the research results based on NTL data. Thus, this article has attempted to propose a new spectral index—the points of interest, road network and EVI adjusted NTL index (PREANTLI) to effectively correct saturated pixels. To evaluate the desaturation effect, the PREANTLI was compared with existing saturation correction data across three aspects: the capacity to display differences in light intensities; the similarity with National Polar-orbiting Partnership/Visible Infrared Imaging Radiometer Suite (NPP/VIIRS) data; and the capacity to estimate the gross domestic product (GDP) and electric power consumption (EPC). The results showed that the PREANTLI can more easily identify light intensity differences than other indexes. The PREANTLI presents a strong linear correlation with the NPP/VIIRS data and socioeconomic statistics (GDP and EPC) at provincial and municipal scales. It is worth noting that, on the pixel scale, the correlation between PREANTLI and NPP/VIIRS ($R^2 = 0.63$) is far higher than that of the other two existing saturation correction index whose R^2 are both below 0.45. Thus, the PREANTLI can be considered as a reasonable index that is not only easy to calculate but can also better alleviate light intensity saturation and emphasize light differences within a city than other indexes.**

***Index Terms*—China, defense meteorological satellite program-operational line-scan system (DMSP-OLS), nighttime light data, saturated light correction, social sensing data.**

Manuscript received August 28, 2020; revised November 12, 2020 and December 12, 2020; accepted January 4, 2021. Date of publication January 8, 2021; date of current version January 27, 2021. This work was supported in part by the Ministry of Education in China Project of Humanities and Social Sciences under Garnt 18XJC790011, in part by the Fundamental Research Founds for the Central Universities under Grant XDJK2020B008, and in part by the Municipal Training Program of Innovation and Entrepreneurship for Undergraduates of Chongqing under Grant S202010635067. *(Corresponding author: Kaifang Shi.)*

Xiaolei Huang, Kaifang Shi, and Yuanqing Li are with the School of Geographical Sciences, State Cultivation Base of Eco-agriculture for Southwest Mountainous Land, Southwest University, Chongqing 400715, China, with the Chongqing Jinfo Mountain Karst Ecosystem National Observation and Research Station, Southwest University, Chongqing 400715, China, and also with the Chongqing Engineering Research Centre for Remote Sensing Big Data Application, School of Geographical Sciences, Southwest University, Chongqing 400715, China (e-mail: shikf1986@126.com; xl1999@email.swu.edu.cn; xslyq@swu.edu.cn).

Yuanzheng Cui is with the Laboratory of Watershed Geographic Sciences, Nanjing Institute of Geography and Limnology, The Chinese Academy of Sciences, Nanjing 210008, China, and also with the Department of Geography and Resource Management, The Chinese University of Hong Kong, Hong Kong (e-mail: ryancuiyz@zufe.edu.cn).

This article has supplementary downloadable material available at https://doi.org/10.1109/JSTARS.2021.3049829, provided by the authors.

Digital Object Identifier 10.1109/JSTARS.2021.3049829

I. Introduction

The defense meteorological satellite program-operational line-scan system (DMSP-OLS) was originally designed for meteorological monitoring to detect moonlit clouds [1], [2]. Since it can detect weak surface near-infrared radiation at night due to its unique photoelectric amplification ability, nighttime light images obtained by the sensor are gradually used to quantify human activities [3], [4]. DMSP-OLS data synthesized on an annual basis remove the influence of transient luminous events and noise, and the stable data (NTL) formed could be used to characterize human nighttime activities [5]. With the long time span and low acquisition cost of NTL data, they are widely used in urbanization evaluation [6]–[10], spatial structure analysis of urban agglomeration [11], [12], and estimation of socioeconomic indicators [3], [13], [14]. However, since the sensor is not equipped with an on-orbit calibration system, the dynamic range of the digital number (DN) is limited to 0–63, which results in oversaturation of the data when describing the actual light intensity on the surface, especially in urban centers with high light intensity at night [15]. The defect of oversaturation limits the upper limit of the actual light intensity, weakening the description of the differences in the light details in the saturated area, and the loss of light details will inevitably reduce the accuracy [16]. Therefore, effective correction of the saturation to obtain high-precision NTL data is an important research topic.

To alleviate the saturation problem, researchers have proposed two kinds of methods: radiative calibration and nonradiative calibration [17]–[21]. The radiation calibration method is relatively perfect in theory and highly accurate in practice. However, the National Geophysical Data Center (NGDC) has only developed a few radiation calibration data products for specific periods due to the lack of satellite calibration systems in the OLS visible band, the complexity of the calibration algorithm, and the large amount of data needed to support it. To compensate for this deficiency, researchers have made many attempts at non-radiative calibration, which can be mainly divided into two types: cross-correction based on radiance-calibrated nighttime light in the invariant target area and association correction based on auxiliary data or parameters. For example, Letu *et al*. [18] assumed that the light intensity did not change significantly within a study area from 1996 to 1999 and calculated the actual DN of the light in the saturated area in 1999 by establishing a functional relationship between the DNs of the light in the unsaturated area in 1999 and the DNs of the radiometric calibration image in 1996 and 1997. Wu *et al*. [22] selected a number of invariant target areas distributed around the world and established a power equation for the saturation correction of light images with a radiometric calibration light image from 2006. Cao *et al*. [23] selected the district of Hegang in China as the invariant target area, and established a power equation with the 2006 radiometric calibration light image as the reference for the data correction. These studies assumed that the actual DNs of saturated pixels will hardly change over several years, which be applicable in places with high urbanization levels and stable development (such as the United States, the United Kingdom, and Japan), but is difficult to guarantee in countries with rapid urbanization rates (such as China and India). With the progress of urbanization and the increase in human activities, the representative landscape of the city has gradually changed from the original natural landscape to impervious surfaces; that is, there is a strong negative correlation between the coverage of impervious surfaces and the vegetation coverage—the higher the coverage of impervious surfaces is, the lower the vegetation coverage. Therefore, many studies have introduced vegetation indexes to saturate NTL data. For example, Lu *et al*. [24] has attempted to use the differentiation characteristics of normalized difference vegetation index (NDVI) in the saturated area to correct the problem of saturation of the NTL data. However, the premise is to assume that the NTL intensity and the NDVI are significantly negatively correlated, resulting in the problem of excessive correction. For this reason, Zhang *et al*. [20] constructed a simple and effective light saturation index—the vegetation-adjusted NTL urban index based on the NDVI. Also, Zhuo *et al*. [25] incorporated enhanced vegetation index (EVI) into the saturation correction model as a correction parameter and proposed the lighting correction index—the EVI-adjusted NTL index. The index can alleviate light saturation more effectively than other indexes without increasing the computational complexity. Generally, the application of vegetation remote sensing in saturation correction studies provides a more effective way to study saturation correction of NTL data. Considering that NTL data reflect the intensity of the nighttime lights in the region and are more significantly affected by socioeconomic factors than other data, the saturation results will inevitably have a certain deviation when taking a vegetation index as the saturation correction parameter.

With the development of geospatial big data and smart cities, it is possible to obtain massive geospatial data, and researchers have begun to attempt to introduce social sensing data to desaturate NTL data [26], [27]. Zheng *et al*. [28] proposed the vector-data-adjusted NTL index (VDANTLI) and added point of interest (POI) data and road network data as correction parameters to correct the saturation phenomenon of NTL data in China's Beijing-Tianjin-Hebei, Yangtze River Delta and Pearl River Delta regions. It effectively alleviated the NTL data saturation problem and enhanced the urban light differences. In addition, it further realized the NTL saturation correction results of the spatial resolution series and long time series VDANTLI. However, the social sensing data introduced by the method are vector data, which are distributed sporadically and intermittently in the region, and it is difficult to correct uncovered region. To date, how to effectively correct the DNs of saturated pixels is still an interest topic; however, there are still some defects in existing NTL saturation correction methods, and there are few studies on desaturation correction of long time series NTL data, which need to be enriched and developed.

To address the above deficiencies, taking China mainland as the experimental area, this study has attempted to propose a new spectral index (PREANTLI) from the POI, road network, and EVI for the light saturation correction. The objective is to introduce the EVI, POI, and road network into the desaturation correction model and take a new approach to reduce the saturation effect of NTL data in urban areas without increasing the computational complexity. To verify the effectiveness of the desaturation effect of the PREANTLI, we compared it with the EANTLI [25], VDANTLI [28], and National Polar-orbiting Partnership/Visible Infrared Imaging Radiometer Suite (NPP/VIIRS) data. Also, the PREANTLI index have been effectively applied to the correction of long time series NTL data.[1]

II. Data Sources

NTL data from 1992 to 2013 were obtained from the National Oceanic and Atmospheric Administration's National Geophysical Data Center (NOAA/NGDC). The data are an image synthesized from a year's worth of cloud-free data at a spatial resolution of 30 arc seconds (approximately 1 km). The DNs of the NTL data range from 0 to 63. When the visible/near-infrared radiation of the area is too high, the DN remains at 63 and no longer increases with an increase in radiation; that is, the phenomenon of light data saturation is generated.

NPP/VIIRS data were obtained from cloud-free composites from the Earth Observation Group (EOG) of NOAA/NGDC. The data product is a composite image of the average radiation, which previously used the VIIRS cloud mask to determine cloud cover and filter light data and exclude data affected by stray light reflected by the moon and clouds.

The 2013 EVI is a monthly vegetation index of 1 km resolution from the Moderate Resolution Imaging Spectroradiometer (MODIS) MOD13A3 data and was derived from a website interface at the level-1 and Atmosphere Archive and Distribution System (LAADS) from the NASA Goddard Space Center for the storage of MODIS level-1 data, atmospheric and land data, visible light and infrared radiation level-1 products and land products.

Landsat 8 operational land imager (OLI) remote sensing image data at a spatial resolution of 30 m were obtained from the geospatial data cloud, and the cloud cover of all the selected images was less than 5%.

China's POI and road network data from 2013 were downloaded from OpenStreetMap. In addition, the statistical gross domestic product (GDP) and electric power consumption (EPC) data for provinces and prefecture-level cities in China were collected from the China City Statistical Yearbook. The boundary

[1]The datasets can be freely downloaded via https://pan.baidu.com/s/1gZ-gtYYkqw_m-ZHDUSpSLQ

TABLE I
DESCRIPTION OF THE DATA USED IN THIS ARTICLE

Data	Data description	Year	Source
DMSP-OLS	Annual stable NTL composite data, 1000-m resolution	1992-2013	NOAA/NGDC (http://www.ngdc.noaa.gov/eog/dmsp/downloadV4composites.html)
NPP/VIIRS	Average radiation synthesis without effects of cloud, lightning, and other outliers, 500-m resolution	2013	EOG (https://ngdc.noaa.gov/eog/viirs/download_dnb_composites.html)
EVI	Monthly precipitation data, 1000-m resolution	2013	LAADS (https://ladsweb.modaps.eosdis.nasa.gov)
Landsat 8 OLI	Cloud cover is less than 5%, 30-m resolution	2013	Geospatial Data Cloud (http://www.gscloud.cn/)
POI	Vector point data, including spatial coordinate information and other attribute information	2013	OpenStreetMap (https://download.geofabrik.de/asia/china.html#)
Road network data	Vector line data, including spatial coordinate information and other attribute information	2013	OpenStreetMap (https://download.geofabrik.de/asia/china.html#)
GDP and EPC	Annual statistical data of the GDP (Yuan) and EPC (kWh) for provinces and prefecture-level cities in China	2013	China City Statistical Yearbook (http://navi.cnki.net/KNavi/YearbookDetail?pcode=CYFD&pykm=YJHPP&bh)
Administrative boundary	Shapefile of provinces and prefecture-level cities in China	2013	RESDC (http://www.resdc.cn)

data of provinces and prefecture-level cities in China were extracted from the Resource and Environment Data Cloud Platform (RESDC). A summary of the data used in this article is given in Table I.

III. METHODOLOGY

A. Developing PREANTLI

It has been shown that vegetation abundance is closely and inversely correlated with impervious surfaces [29]–[32]. Some researchers have tried to introduce vegetation indexes to saturate NTL data [20], [24], [25]. However, the negative correlation between vegetation indexes and NTL is not absolutely stable. For example, with the continuous advancement of China's urbanization process, the urban impermeable surface area continues to expand, and the vegetation coverage area has decreased sharply, which inhibits the spatial heterogeneity of vegetation indexes. It is difficult to use a vegetation index with low spatial heterogeneity to correct NTL data in light-saturated areas of urban centers. Considering that NTL data mostly reflect the intensity of nighttime lights, which are more significantly affected by socioeconomic factors, Zheng *et al.* [28] attempted to introduce social sensing data to correct the saturation phenomenon of NTL data. Based on the above analysis, we comprehensively consider natural and socioeconomic factors to correct the NTL saturation phenomena.

Considering that there is a negative correlation between the EVI, human economic, and social activities, and that the EVI has the advantages of overcoming its own saturation and inhibiting soil background interference, this study selected the EVI as the remote sensing data. POI data mainly include some geographical entities closely related to people's activities and urban structure, such as transportation hubs, banks, and restaurants. Thus, POI data are widely used in social and economic fields and are positively correlated with human economic activities. Road network data can depict the development layout of a city on a small scale and can reflect the network structure between pairs of cities and between cities and villages on a medium scale. Moreover, these data are clearly shown linear veins on light intensity maps and are positively correlated with human economic activities. This article also selected POIs and road networks as social sensing data. Therefore, EVI, POI, and road network data were introduced as desaturation parameters to construct the NTL desaturation index, PREANTLI.

To some extent, the mean value is relatively stable; thus, the sensitivity of the PREANTLI to the EVI can be reduced. In this article, the annual mean value of the EVI in 2013 is calculated by using the original monthly mean EVI over 12 months. It is noted that all EVI pixels with values less than 0.01 have been eliminated to avoid the excessive correction caused by the infinite ratio of EVI_{avg} to EVI. The POI data used in this study include 12 categories of basic urban functional facilities, such as catering, enterprise, finance, hotel, residence, and transportation facilities, which can represent the majority of the population and its activities in urban centers. According to the characteristics of various levels of road networks, this article divided the road network data into three categories: urban expressways; urban inner roads; and pedestrian roads. Also, the roads were given different weights based on the analytic hierarchy process (AHP). The general process of AHP is as follows: first, we established a road network weight allocation system on the basis of considering the four principles of road grade level, average road speed, road connectivity, and road congestion. Second, we selected six experienced drivers as experts to set the index weight of each layer, and built a judgment matrix that passed the consistency test after many discussions and revisions. Third, the weight was calculated according to the index weight of each layer. The PREANTLI was calculated as

$$\mathrm{RNDD} = \mathrm{Sum}\left(\mathrm{WL}_{\mathrm{Road\ network}_{\mathrm{level}_{1,2,3}}}\right)$$

$$\mathrm{PREANTLI} = \left(\frac{\mathrm{POI}_{\mathrm{Kernel}}}{\mathrm{POI}_{\mathrm{Kernel}_{\mathrm{avg}}}} + \frac{\mathrm{RNDD}}{\mathrm{RNDD}_{\mathrm{avg}}} + \frac{\mathrm{EVI}_{\mathrm{avg}}}{\mathrm{EVI}}\right)_{\mathrm{norm}} \times \mathrm{NTL}_{\mathrm{norm}} \quad (1)$$

where RNDD is the weight length of the road network in each 1000 $\times$1000 m grid and the road types and weights of the network are as follows: urban expressway (weight: 0.5) $>$ urban inner roads (weight: 0.3) $>$ pedestrian street (weight: 0.2). $\mathrm{POI}_{\mathrm{Kernel}}$ is the result of kernel density analysis for the POI. $\mathrm{NTL}_{\mathrm{nor}}$ is the normalized NTL.$\mathrm{EVI}_{\mathrm{avg}}$, $\mathrm{POI}_{\mathrm{Kernel}_{\mathrm{avg}}}$, and $\mathrm{RNDD}_{\mathrm{avg}}$ are the mean values of the EVI, $\mathrm{POI}_{\mathrm{Kernel}}$ and RNDD in the potential light-saturated area (the area where the DN equals 63).

B. Accuracy Verification

First of all, we evaluated the ability of the PREANTLI to reduce the NTL saturation by quantitatively and qualitatively comparing with the EANTLI and VDANTLI that have widely been accepted and proved to be effective for saturation correction [25], [28]. Considering that the VIIRS is more sensitive to NTL than other sensors and that there is no pixel saturation problem in the NPP/VIIRS data, which can more accurately reflect the spatial information of human economic activities, we also selected outlier-free NPP/VIIRS data as the standard effect for the comparative verification. To facilitate the comparison, the original NTL data, the desaturation correction results of the three indicators and the NPP/VIIRS data were normalized to the range of [0, 1]. The qualitative comparison verification step was carried out from both the horizontal and vertical aspects. First, we compared and observed the light intensity differences of the PREANTLI, EANTLI, VDANTLI, NTL, and NPP/VIIRS with Landsat 8 data from the same year. Then, we further compared the transects of the PREANTLI, EANTLI, VDANTLI, NTL, and NPP/VIIRS data in Wuhan, Tianjin and Ningbo to compare the capabilities of each index to display light details in light-saturated areas.

To further quantify the similarity between the three saturation correction indicators and the standard NPP/VIIRS image, we carried out a regression analysis between the NTL, PREANTLI, EANTLI, VDANTLI, and NPP/VIIRS data at the provincial, municipal, and pixel levels, respectively. Considering the high correlation between NTL data and socioeconomic indicators, we carried out regression analysis between the NTL, PREANTLI, EANTLI, VDANTLI, NPP/VIIRS, and socioeconomic indicators (GDP and EPC) at the provincial and municipal levels.

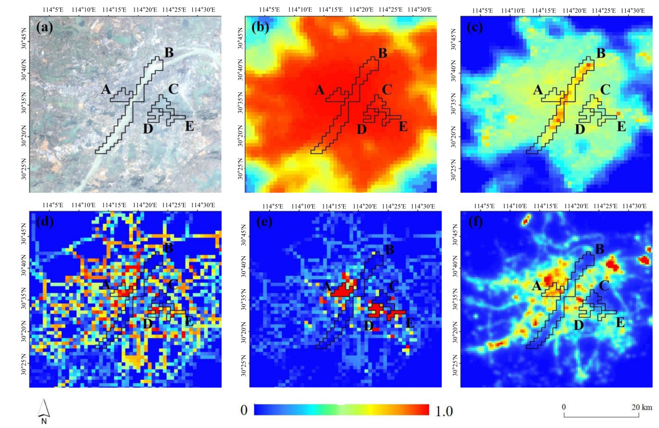

Fig. 1. Normalized nighttime light images for the selected sample regions in Wuhan. (a) Landsat 8. (b) NTL. (c) EVI-adjusted NTL index. (d) Vector-data-adjusted NTL index. (e) The points of interest, road network, and EVI adjusted NTL index. (f) National Polar-orbiting Partnership/Visible Infrared Imaging Radiometer Suite.

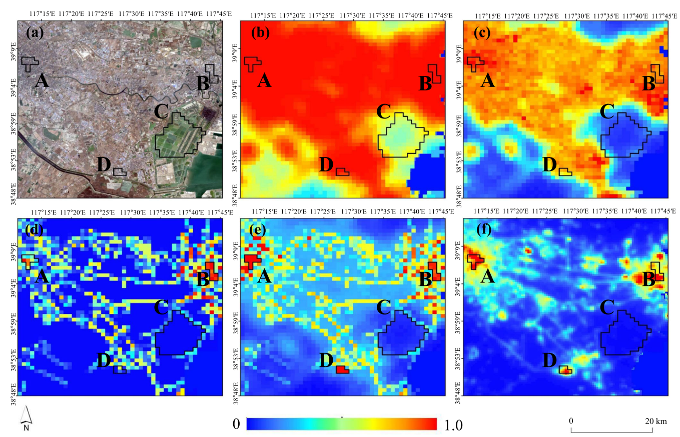

Fig. 2. Normalized nighttime light images for the selected sample regions in Tianjin. (a) Landsat 8. (b) NTL. (c) EVI-adjusted NTL index. (d) Vector-data-adjusted NTL index. (e) The points of interest, road network, and EVI adjusted NTL index. (f) National Polar-orbiting Partnership/Visible Infrared Imaging Radiometer Suite.

IV. Results and Discussion

A. Comparison of the Capacity to Display Differences in Light Intensity

Wuhan, Tianjin, and Ningbo were selected as experimental examples, because the saturation phenome in these cities was more easily affected by rivers, lakes, or other natural factors than that of some typical large cities, such as Beijing and Shanghai. We carried out a comparative analysis of the PREANTLI, EANTLI, VDANTLI, NTL, and NPP/VIIRS data from the horizontal and vertical aspects. The abilities of the EANTLI, VDANTLI, PREANTLI, NTL, and NPP/VIIRS indicators to identify surface features in the urban interior were compared and analyzed with the Landsat 8 reference data from the same year (see Figs. 1 –3). Also, Beijing and Guangzhou were selected as validation examples. Due to layout

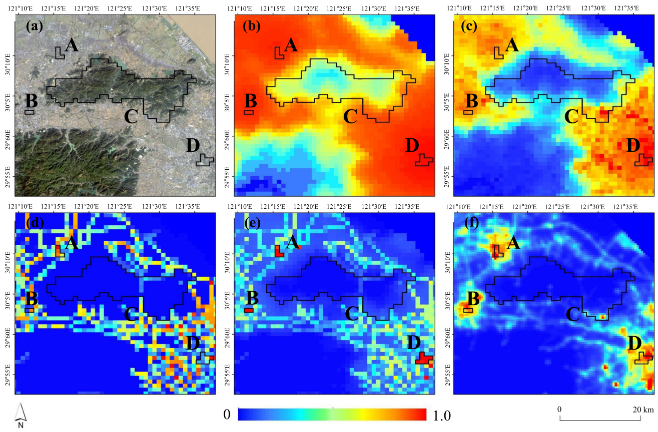

Fig. 3. Normalized nighttime light images for the selected sample regions in Ningbo. (a) Landsat 8. (b) NTL. (c) EVI-adjusted NTL index. (d) Vector-data-adjusted NTL index. (e) The points of interest, road network, and EVI adjusted NTL index. (f) National Polar-orbiting Partnership/Visible Infrared Imaging Radiometer Suite.

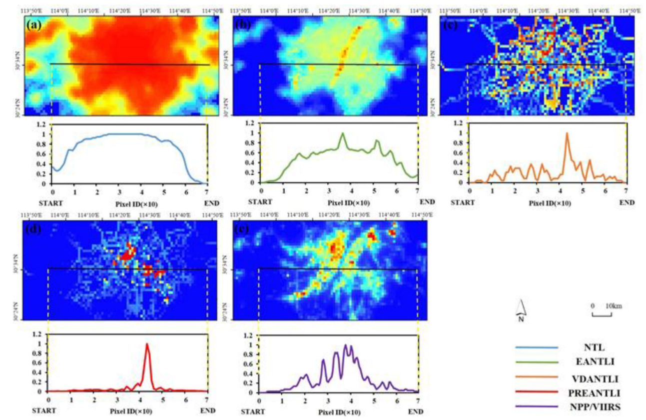

Fig. 4. Transect passing through the potentially saturated areas of Wuhan. (a) NTL. (b) EVI-adjusted NTL index. (c) Vector-data-adjusted NTL index. (d) The points of interest, road network, and EVI adjusted NTL index. (e) National Polar-orbiting Partnership/Visible Infrared Imaging Radiometer Suite.

restrictions. The corresponding results are shown in figures S1 and S2.

As shown in Fig. 1, the PREANTLI can identify the Jianghan District of the Wuhan city economic center, the Yangtze River and East Lake, and Hongshan District universities, which is similar to the NPP/VIIRS data. However, the EANTLI miscalculated the Yangtze River as having a high NTL value, and it was difficult to identify the areas of high and low values of light. The VDANTLI recognized the Yangtze River and East Lake, but it had difficulty recognize economically developed areas (high-light areas) due to the fragmented light areas.

Fig. 2 also suggested that the PREANTLI can better identify the peace district economic center, the coastal new area economic center, the cultivated land area, and the oil and chemical industry area; it is still difficult for the EANTLI to identify features in the potential saturation zone. The VDANTLI can distinguish ground objects in the saturated area, but it still has difficult identifying the high-value light area. Moreover, by comparing the VDANTLI with the NPP/VIIRS data, it can be seen that in many areas where lights should exist, the DN from the VDANTLI is corrected to zero, which is obviously inconsistent with reality.

From Fig. 3, the PREANTLI better identifies the Cixi Economic Center, the Yuyao Economic Center, the Five Lei Mountain Scenic Spot, and Haishu District Economic Center. The PREANTLI is similar to the NPP/VIIRS data and continues to maintain its advantage of object recognition.

It can be seen from the above analysis that the EANTLI, VDANTLI, and PREANTLI have all corrected the oversaturation problem of the original NTL data to emphasize the interior light details of the saturated area, but the effects of the three indexes are obviously different. Among them, the EANTLI has the worst desaturation correction effect. It has difficulty distinguishing the differences in NTL in the saturated area and identify the ground objects in the saturated area, and the DN of the water area is incorrectly calculated as a large value. The EANTLI was calculated according to the trend of negative correlation between vegetation and human activities. However, with the expansion and development of urbanization, urban coverage is gradually replaced by impermeable surfaces, so the difference in urban vegetation coverage is not obvious. Therefore, it is difficult to distinguish the light differences in the urban interior from the desaturation correction result of the EANTLI. Additionally, the EANTLI incorrectly stretched the DN of the water area because of the low EVI value in the water area. The ability of the VDANTLI to distinguish ground objects in the saturated area is better than that of the EANTLI. However, the ground objects recognized by the calibration results are too fragmented to identify the areas with high and low values for lights in the saturated area and extract their regularity. In addition, the VDANTLI incorrectly corrected the DNs to 0 in many areas that should have light. The VDANTLI is calculated according to the trend that the POI density and road network length are positively correlated with human activities. However, for areas without POI and road network coverage, its DN is wrongly corrected to 0, which is obviously inconsistent with reality. Urban nighttime lights are mainly influenced by socioeconomic factors, but the impact of natural factors cannot be ignored. The desaturation correction model PREANTLI combined with POI, road network, and EVI data highlights the details of urban interior lights well and is closer to the NPP/VIIRS data than the other indexes.

Also, we further compared the transect of the PREANTLI, EANTLI, VDANTLI, NTL, and NPP/VIIRS data in Wuhan, Tianjin, and Ningbo to compare their capabilities to display the light detail in the light-saturated areas, and the results are shown in Figs. 4–6.

As shown in Fig. 4, the EANTLI, VDANTLI, and PREANTLI all enhanced the light details compared with the original NTL saturation region of the Wuhan region, but the EANTLI enhancement effect is not good. Both the VDANTLI and PREANTLI show good light detail and are similar to the NPP/VIIRS data. By contrast, the increasing-decreasing trend shown by the

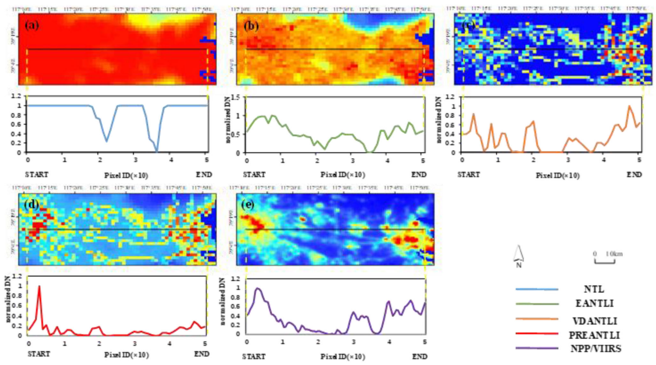

Fig. 5. Transect passing through the potentially saturated areas of Tianjin. (a) NTL. (b) EVI-adjusted NTL index (c) Vector-data-adjusted NTL index. (d) The points of interest, road network, and EVI adjusted NTL index. (e) National Polar-orbiting Partnership/Visible Infrared Imaging Radiometer Suite.

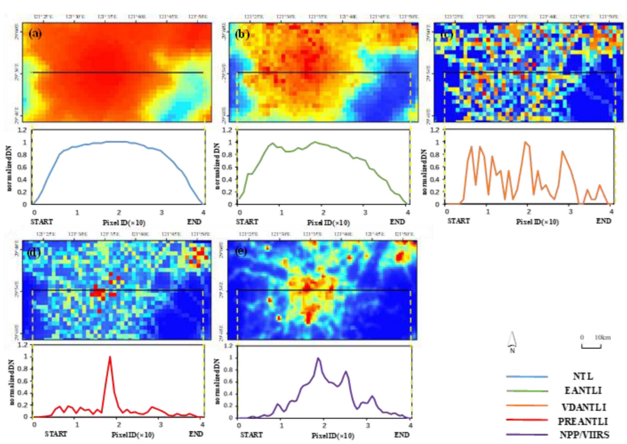

Fig. 6. Transect passing through the potentially saturated areas of Ningbo. (a) NTL. (b) EVI-adjusted NTL index. (c) Vector-data-adjusted NTL index. (d) The points of interest, road network, and EVI adjusted NTL index. (e) National Polar-orbiting Partnership/Visible Infrared Imaging Radiometer Suite.

PREANTLI is closer to that of the NPP/VIIRS data, and the PREANTLI highlights the primary economic center (the area with the largest brightness) better than the other indexes.

As shown in Fig. 5, the effect of the EANTLI in displaying the light details is still not good. The PREANTLI shows that the primary economic center of this cross-sectional line in the Tianjin region is located between pixels 0–10 and is consistent with the NPP/VIIRS data, while the VDANTLI shows that the primary economic center is located between pixels 40 and 50, inconsistent with the NPP/VIIRS data.

As shown in Fig. 6, the EANTLI is still not good at showing the lighting details. The PREANTLI obtains lighting details of the cross-sectional line in the Ningbo region similar to those of the NPP/VIIRS data, while the VDANTLI misjudges the area of low values between pixels 0 and 15 and around pixel 30 as an area with high values, and it has difficulty in identifying the location of the economic center.

According to the above analysis, we found that the EANTLI has a poor ability to display lighting details. The desaturation

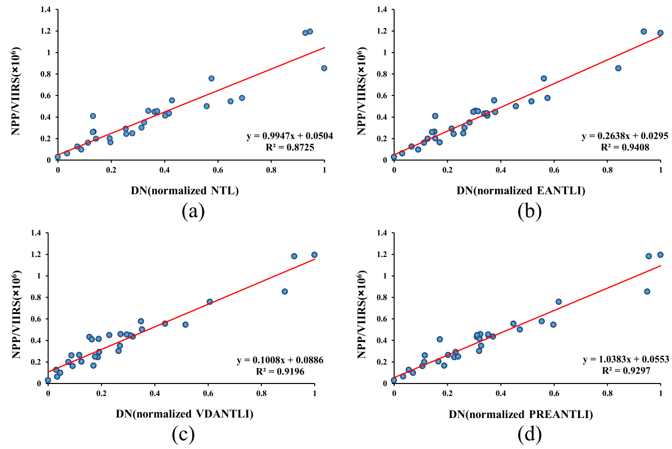

Fig. 7. Regression analysis with the NPP/VIIRS data at the provincial level. (a) NTL. (b) EVI-adjusted NTL index. (c) Vector-data-adjusted NTL index. (d) The points of interest, road network, and EVI adjusted NTL index.

results of the VDANTLI and PREANTLI emphasize the light details in the light saturation region well, but the VDANTLI overstretches the low-value region of light, which leads to problems such as difficulty identifying or misjudging the primary economic center. For example, in natural scenic areas where POIs and roads are concentrated, the introduction of POI and road network data as correction parameters leads to overstretching, resulting in the incorrect correction of the low-light area to the high-light area. If the EVI is introduced into the modified model at this time, the problem of overstretching can be remedied. It can also be seen in Figs. 6 and 7 that the PREANTLI, which introduces POI, road network, and EVI data into the desaturation correction model, is consistent with the NPP/VIIRS data, which verifies the ability of the PREANTLI to display light details in the saturated region.

B. Comparison of the Similarity With the NPP/VIIRS Data

To evaluate the ability of the PREANTLI to correct saturation issue, this study fitted the EANTLI, VDANTLI, and PREANTLI with NPP/VIIRS nighttime light data at the provincial, municipal and pixel levels and then quantitatively analyzed and evaluated the desaturation correction ability of the PREANTLI. The results are shown in Figs. 7–9 and Table II.

As shown in Figs. 7 and 8, the fitting degrees of the EANTLI, VDANTLI, PREANTLI, and NTL data compared with the NPP/VIIRS data at the provincial and municipal levels. Among them, the fitting degree of the PREANTLI and the NPP/VIIRS data ($R^2 = 0.930$) is between that of the EANTLI and the NPP/VIIRS data ($R^2 = 0.941$) and that of the VDANTLI and the NPP/VIIRS data ($R^2 = 0.920$) at the provincial level. All three fitting degrees are at a high level. At the municipal level, the fitting degree between the PREANTLI and the NPP/VIIRS data ($R^2 = 0.864$) and between the EANTLI the NPP/VIIRS data ($R^2 = 0.878$) was significantly higher than that between the VDANTLI and the NPP/VIIRS data ($R^2 = 0.812$).

As shown in Fig. 9 and Table II, on the pixel level, the fitting degree between the PREANTLI and the NPP/VIIRS data ($R^2 =$

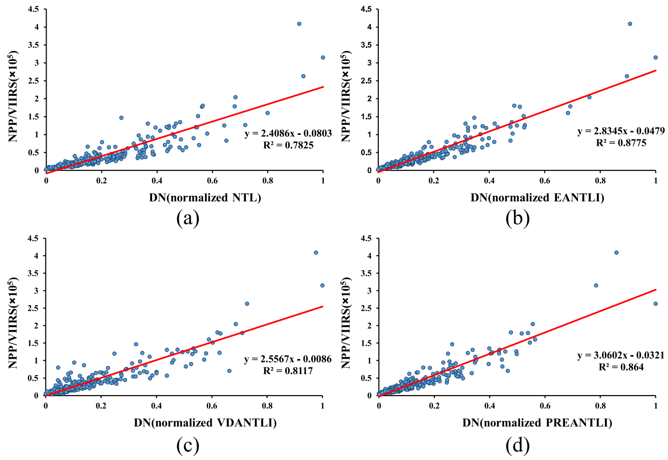

Fig. 8. Regression analysis with the NPP/VIIRS data at the municipal level. (a) NTL. (b) EVI-adjusted NTL index. (c) Vector-data-adjusted NTL index. (d) The points of interest, road network, and EVI adjusted NTL index.

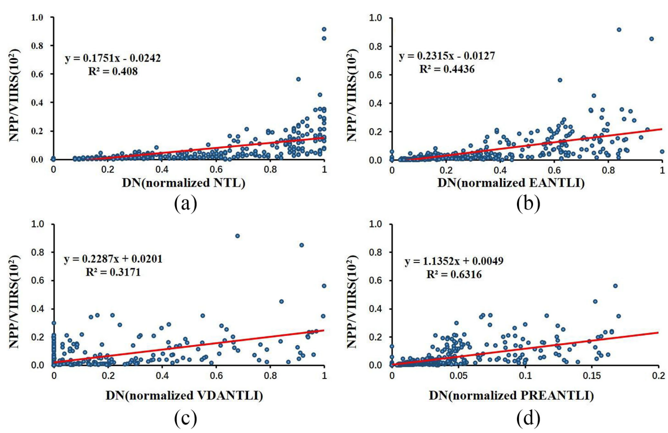

Fig. 9. Regression analysis with the NPP/VIIRS data at the pixel level. (a) NTL. (b) EVI-adjusted NTL index. (c) Vector-data-adjusted NTL index. (d) The points of interest, road network, and EVI adjusted NTL index.

TABLE II
RESULTS OF REGRESSION ANALYSIS OF THE NTL, EANTLI, VDANTLI, AND PREANTLI WITH THE NPP/VIIRS DATA AT THE PIXEL LEVEL IN WUHAN, TIANJIN, AND NINGBO

City	Data	Fitted function	R^2
Wuhan	NTL	y=0.2983x-0.0284	0.537
	EANTLI	y=0.3669x-0.0143	0.554
	VDANTLI	y=0.4820x+0.0211	0.524
	PREANTLI	y=0.6798x-0.0041	0.588
Tianjin	NTL	y=0.1984x-0.0368	0.345
	EANTLI	y=0.2427x-0.0186	0.418
	VDANTLI	y=0.3530x+0.0229	0.342
	PREANTLI	y=1.1492x-0.0082	0.732
Ningbo	NTL	y=0.2063x-0.0299	0.379
	EANTLI	y=0.2392x-0.0176	0.398
	VDANTLI	y=0.1870x+0.0269	0.239
	PREANTLI	y=1.0277x+0.0114	0.681

TABLE III
RESULTS OF REGRESSION ANALYSIS OF THE NTL, EANTLI, VDANTLI, AND PREANTLI WITH THE GDP AND EPC AT THE PROVINCIAL LEVEL

Economic indicator	Data	Fitted function	R^2
GDP	NTL	y=5.1895x+0.1684	0.778
	EANTLI	y=5.7848x+0.1561	0.850
	VDANTLI	y=5.6912x+0.4013	0.888
	PREANTLI	y=5.5248x+0.1574	0.863
	NPP/VIIRS	y=5.9787x+0.1332	0.880
EPC	NTL	y=4.3219x+0.1711	0.850
	EANTLI	y=4.7358x+0.1874	0.897
	VDANTLI	y=4.4821x+0.4388	0.868
	PREANTLI	y=4.4693x+0.2066	0.889
	NPP/VIIRS	y=4.8272x+0.1640	0.885

TABLE IV
RESULTS OF REGRESSION ANALYSIS OF THE NTL, EANTLI, VDANTLI, AND PREANTLI WITH THE GDP AND EPC AT THE MUNICIPAL LEVEL

Economic indicator	Data	Fitted function	R^2
GDP	NTL	y=1.2651-0.0386	0.639
	EANTLI	y=1.5014x-0.0241	0.735
	VDANTLI	y=1.3932x-0.008	0.688
	PREANTLI	y=0.2088x-0.0537	0.753
	NPP/VIIRS	y=2.1285x+0.0202	0.828
EPC	NTL	y=0.1577x-0.035	0.428
	EANTLI	y=0.6855x-0.0176	0.530
	VDANTLI	y=0.6485x-0.0123	0.516
	PREANTLI	y=0.0956x-0.0315	0.548
	NPP/VIIRS	y=1.0432x-0.0041	0.689

0.632) is much higher than that between the original NTL ($R^2 = 0.408$), EANTLI ($R^2 = 0.444$), and VDANTLI ($R^2 = 0.317$) and the NPP/VIIRS data. The PREANTLI has a high degree of similarity with the NPP/VIIRS data from a quantitative perspective, which is consistent with the coherence of the PREANTLI and NPP/VIIRS at the pixel level in the aforementioned qualitative analysis. This article provides a new idea for the joint application of NTL data with NPP/VIIRS data.

C. Comparison of the Capacity to Estimate the GDP and EPC

The GDP and EPC were also used in our study to conduct correlation analysis with the NTL, EANTLI, VDANTLI, PREANTLI, and NPP/VIIRS data at the provincial and municipal levels. The total DN of each prefecture-level city or province is calculated by the Zonal Statistics as Table tool in ArcGIS 10.5, and the results are shown in Tables III and IV; and Figs. 10 and 11.

As given in Table III, at the provincial level, the fitting degree of the PREANTLI and the GDP ($R^2 = 0.863$) is between that of the EANTLI and the GDP ($R^2 = 0.850$) and that of the VDANTLI and the GDP ($R^2 = 0.888$) and slightly lower than that of the VDANTLI and the GDP. The fitting degree of the PREANTLI with the EPC ($R^2 = 0.889$) is also between that of the EANTLI and the EPC ($R^2 = 0.897$) and that of the VDANTLI

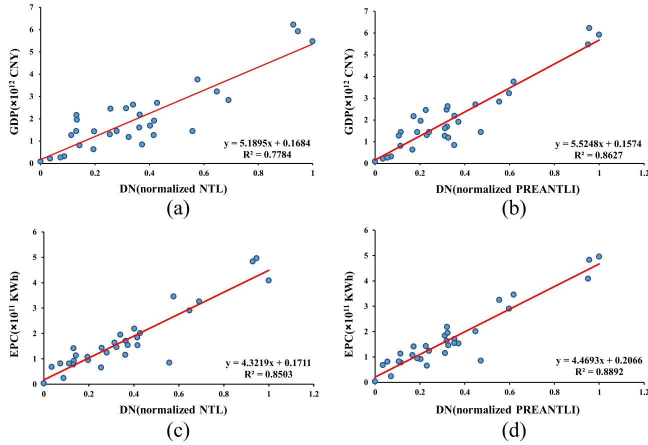

Fig. 10. Regression analysis with the GDP and EPC at the provincial level. (a) NTL versus gross domestic product. (b) The points of interest, road network, and EVI adjusted NTL index versus gross domestic product. (c) NTL versus electric power consumption. (d) The points of interest, road network, and EVI adjusted NTL index versus electric power consumption.

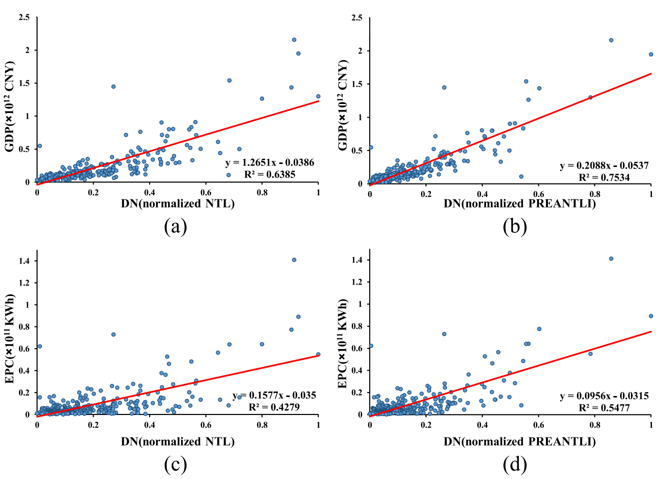

Fig. 11. Regression analysis with the GDP and EPC at the municipal level. (a) NTL versus gross domestic product. (b) The points of interest, road network, and EVI adjusted NTL index versus gross domestic product. (c) NTL versus electric power consumption. (d) The points of interest, road network, and EVI adjusted NTL index versus electric power consumption.

and the EPC ($R^2 = 0.868$) and slightly lower than that of the EANTLI and the EPC.

As given in Table IV, at the municipal level, the fitting degree of the PREANTLI and the GDP ($R^2 = 0.753$) was significantly higher than that of the VDANTLI and the GDP ($R^2 = 0.688$) and slightly higher than that of the EANTLI and the GDP ($R^2 = 0.735$). The fitting degree of the PREANTLI and the EPC ($R^2 = 0.548$) was also higher than that of the EANTLI and the EPC ($R^2 = 0.530$) and that of the VDANTLI and the EPC ($R^2 = 0.516$). Therefore, it can be seen that the PREANTLI has a better fitting effect with these socioeconomic statistics at the provincial and municipal levels and has a great advantage over the EANTLI and VDANTLI.

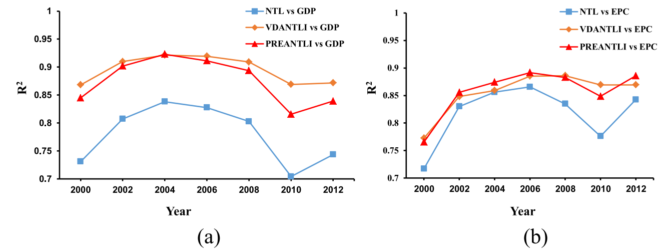

Fig. 12. Fitting results of the NTL, VDANTLI, and PREANTLI datasets with (a) GDP and (b) EPC at the provincial level from 2000 to 2012.

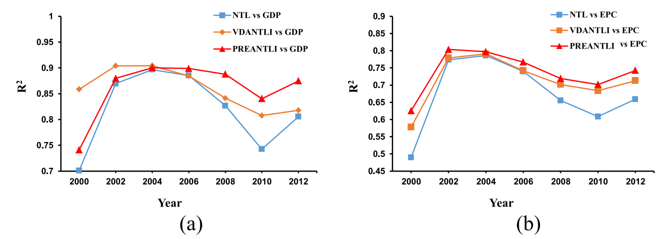

Fig. 13. Fitting results of the NTL, VDANTLI, and PREANTLI datasets with (a) GDP and (b) EPC at the municipal level from 2000 to 2012.

D. *Evaluation of the Desaturation Effect of the PREANTLI Datasets*

Based on the accuracy verification in Section IV-A–Section IV-C, we found that the PREANTLI has a better saturation correction effect than the other indexes, whether in the aspect of identifying features and displaying the light details qualitatively or in the aspect of fitting degree with the NPP/VIIRS data and fitting degree with socioeconomic statistical data (the GDP and EPC). It can eliminate the saturation defect of the original NTL data, and it has more advantages than the EANTLI and VDANTLI. Considering that DMSP-OLS provides a series of annual cloudless nighttime light images and its ability to observe earth in large scale and long time series effectively supports the study of human activities on the surface and urbanization process. We attempted to construct long-term series of NTL with PREANTLI and verify its accuracy.

Before desaturation, the acquired NTL time series images need to be preprocessed to eliminate the obvious DN fluctuation anomalies of from different sensors in the same year or from the same sensor in different years. We used the invariant target area correction method proposed by Elvidge *et al.* [33] to improve the continuity and comparability of the NTL data. However, due to the lack of road network and POI data before 2013, we tried to use the single-period vector dataset as an auxiliary parameter to correct the native NTL time series image

To verify the availability of PREANTLI datasets, we analyzed the fitting degree of the original NTL dataset and the VDANTLI dataset constructed by Zheng *et al.* [28] with the socioeconomic time series statistics of at the provincial and municipal levels, and the results are shown in Figs. 12 and 13, respectively.

As shown in Fig. 12, the fitting degree of the PREANTLI and VDANTLI datasets is close to that of the socioeconomic statistics at the provincial level. Fig. 12(a) shows that the fitting degree of the PREANTLI and the GDP was slightly lower than that of the VDANTLI and the GDP in 2000, 2002 and 2006 but slightly higher than that of the VDANTLI and the GDP in 2010 and 2012. Fig. 12(b) shows that the fitting degree of the PREANTLI and the EPC was slightly lower than that of the VDANTLI and the EPC in 2000 and 2010 but slightly higher than that of the VDANTLI and the EPC in 2002, 2004, 2006, and 2012.

As shown in Fig. 13, the degree of fitting between the PREANTLI and VDANTLI datasets with the socioeconomic statistics is generally better than that of the NTL dataset at the municipal level. In addition, it can be seen from Fig. 13(b) that the fitting degree of the VDANTLI and the EPC did not improve compared with the original NTL, with no correction effect from 2002 to 2006.

Therefore, the comparison of the fitting degree between the PREANTLI and VDANTLI datasets with the socioeconomic statistics at the provincial and municipal levels shows that the PREANTLI datasets constructed in this study have more advantages than the other data.

E. Limitations and Future Directions

Although the results of our study show that the PREANTLI has a certain effect on the saturation correction of the NTL data, the desaturation correction method still needs further research. First, the accuracy of the PREANTLI partly depends on the quality of the POI data (including its quantity, distribution and type) to a certain extent. However, in cities of different urbanization levels or in different areas of the same city, the update frequency of the POI data is not consistent. Generally, the higher the urbanization level of a city, the more the city center represents the city, and the faster the POI data are updated. Second, we subjectively divided road networks into urban expressways, urban inner roads, and pedestrian roads based on the road type and weighted them ((urban expressway (weight: 0.5) > urban inner road (weight: 0.3) > pedestrian road (weight: 0.2)). However, whether there is a better classification and weighting method to produce a better desaturation effect and better reflect the inner details of the city center still needs further research. In a follow-up study, the PREANTLI can be combined with other data, such as surface temperature data, GDP data, and population data, to provide more methods and directions for NTL desaturation research.

V. Conclusion

This article has attempted to propose a saturated light correction method for NTL data from remote sensing (EVI) and social sensing data (POIs and road networks). First, from a qualitative perspective, we used high-resolution Landsat 8 images to compare three saturated light correction data in their ability to identify surface features and their ability to display light details based on the transect passing through the saturated area. Second, from a quantitative perspective, we analyzed the fitting degree of the three methods with NPP/VIIRS data without outliers, and then we analyzed the fitting degree of the three methods with socioeconomic data (the GDP and EPC) at the provincial and municipal levels. In both the qualitative and quantitative analyses, the desaturation effect of the PREANTLI on NTL has been proved to be better than that of the EANTLI and VDANTLI, which indicates that the PREANTLI desaturation method based on remote (EVI) and social sensing data (POIs and road networks) has certain feasibility. Moreover, considering the approximate computational complexity of the three indexes, the PREANTLI is more advantageous for the desaturation of NTL data. The PREANTLI provides a method based on a simple model to produce a better NTL saturation correction effect than previous indexes, which is worth extending.

References

[1] C. D. Elvidge, K. E. Baugh, M. Zhizhin, and F.-C. Hsu, “Why VIIRS data are superior to DMSP for mapping nighttime lights,” *Proc. Asia-Pac. Adv. Netw.*, vol. 35, pp. 62–69, 2013.

[2] C. D. Elvidge, K. E. Baugh, E. A. Kihn, H. W. Kroehl, and E. R. Davis, “Mapping city lights with nighttime data from the DMSP operational linescan system,” *Photogrammetric Eng. Remote Sens.*, vol. 63, no. 6, pp. 727–734, 1997.

[3] C. D. Elvidge, K. E. Baugh, E. Kihn, H. W. Kroehl, E. R. Davis, and C. W. Davis, “Relation between satellite observed visible-near infrared emissions, population, economic activity and electric power consumption,” *Int. J. Remote Sens.*, vol. 18, no. 6, pp. 1373–1379, 1997.

[4] X. Li, C. Elvidge, Y. Zhou, C. Cao, and T. Warner, “Remote sensing of night-time light,” *Int. J. Remote Sens.*, vol. 38, no. 21, pp. 5855–5859, 2017.

[5] X. Li and Y. Zhou, “Urban mapping using DMSP/OLS stable night-time light: A review,” *Int. J. Remote Sens.*, vol. 38, no. 21, pp. 6030–6046, 2017.

[6] J. Chen *et al.*, “The study on urbanization process in China based on DMSP/OLS data: Development of a light index for urbanization level estimation,” (in Chinese), *J. Remote Sens.*, vol. 7, no. 3, pp. 168–175, 2003..

[7] Q. Zhang and K. C. Seto,“Mapping urbanization dynamics at regional and global scales using multi-temporal DMSP/OLS nighttime light data,” *Remote Sens. Environ.*, vol. 115 no. 9, pp. 2320–2329, 2011.

[8] M. Imhoff, L. Tucker, and J. Compton, “The use of multisource satellite and geospatial data to study the effect of urbanization on primary productivity in the United States,” *IEEE Trans. Geosci. Remote Sens.*, vol. 38, no. 6, pp. 2549–2556, Nov. 2000.

[9] B. Yu *et al.*, “Urban built-up area extraction from log-transformed NPP-VIIRS nighttime light composite data,” *IEEE Geosci. Remote Sens. Lett.*, vol. 15, no. 8, pp. 1279–1283, Aug. 2018.

[10] K. Shi *et al.*, “Modeling and mapping total freight traffic in China using NPP-VIIRS nighttime light composite data,” *GISci. Remote Sens.*, vol. 52, no. 3, pp. 274–289, 2015.

[11] C. Small, F. Pozzi, and C. D. Elvidge, “Spatial analysis of global urban extent from DMSP-OLS night lights,” *Remote Sens. Environ.*, vol. 96, no. 3, pp. 277–291, 2005.

[12] P. Xu, P. Jin, Y. Yang, and Q. Wang, “Evaluating urbanization and spatial-temporal pattern using the DMSP/OLS nighttime light data: A case study in Zhejiang province,” *Math. Problems Eng.*, vol. 2016, pp. 1–8, 2016.

[13] S. Amaral, G. Camara, A. Miguel, V. Monteiro, J. A. Quintanilha, and C D. Elvidge, “Estimating population and energy consumption in Brazilian Amazonia using DMSP night-time satellite data,” *Comput. Environ. Urban Syst.*, vol. 29, no. 2, pp. 179–195, 2005.

[14] Y. Xie and Q. Weng, “World energy consumption pattern as revealed by DMSP-OLS nighttime light imagery,” *GISci. Remote Sens.*, vol. 33, no. 2, pp. 265–282, 2015.

[15] K. Shi *et al.*, “Detecting spatiotemporal dynamics of global electric power consumption using DMSP-OLS nighttime stable light data,” *Appl. Energy*, vol. 184,pp. 450–463, 2016.

[16] C. He, Q. Ma, Z. Liu, and Q. Zhang, “Modeling the spatiotemporal dynamics of electric power consumption in Mainland China using saturation corrected DMSP/OLS nighttime stable light data,” *Int. J. Digit. Earth*, vol. 6, no. 1, pp. 1–22, 2013.

[17] C. D. Elvidge, K. E. Baugh, J. B. Dietz, T. Bland, P. C. Sutton, and H. W. Kroehl, “Radiance calibration of DMSP-OLS low-light imaging data of human settlements,” *Remote Sens. Environ.*, vol. 68, no. 1, pp. 77–88, 1999.

[18] H. Letu, M. Hara, G. Tana, and F. Nishio, "A saturated light correction method for DMSP/OLS nighttime satellite imagery," *IEEE Trans. Geosci. Remote Sens.*, vol. 50, no. 2, pp. 389–396, Feb. 2012.

[19] H. Letu*et al.*, "Estimating energy consumption from night-time DMPS/OLS imagery after correcting for saturation effects," (in Chinese), *J. Remote Sens.*, vol. 31, no. 16, pp. 4443–4458, 2010.

[20] Q. Zhang, C. B. Schaaf, and K. C. Seto, "The vegetation adjusted NTL urban index: A new approach to reduce saturation and increase variation in nighttime luminosity," *Remote Sens. Environ.*, vol. 129, pp. 32–41, 2013.

[21] N. Levin *et al.,* "Remote sensing of night lights: A review and an outlook for the future," *Remote Sens. Environ.*, vol. 237, 2020, Art. no. 111443.

[22] J. Wu, S. He, J. Peng,W. Li, and X. Zhong, "Intercalibration of DMSP-OLS night-time light data by the invariant region method," *Int. J. Remote Sens.*, vol. 34, no. 20, pp. 7356–7368, 2013.

[23] Z. Cao,, "Correction of DMSP/OLS night-time light images and its application in China," (in Chinese) , *J. Geo-Inf. Sci.*, vol. 17, no. 9, pp. 1092–1102, 2015.

[24] D. Lu, H. Tian, G. Zhou, and H. Ge, "Regional mapping of human settlements in southeastern China with multisensor remotely sensed data," *Remote Sens. Environ.*, vol. 112, no. 9, pp. 3668–3679, 2008.

[25] L. Zhuo, X. Zhang, J. Zheng, X. Ye, G. Guo, and Q. Qian, "An EVI-based method to reduce saturation of DMSP/OLS nighttime light data," (in Chinese), *Acta Geographica Sinca*, vol. 70, pp. 1339–1350, 2015.

[26] C. He, B. Gao, Q. Huang, Q. Ma, and Y. Dou, "Environmental degradation in the urban areas of China: Evidence from multi-source remote sensing data," *Remote Sens. Environ.*, vol. 193, pp. 65–75, 2017.

[27] K. Shi, Z. Chang, Z. Chen, J. Wu, and B. Yu, "Identifying and evaluating poverty using multisource remote sensing and point of interest (POI) data: A case study of Chongqing, China," *J. Cleaner Prod.*, vol. 255, 2020, Art. no. 120245.

[28] Z. Zheng, Y. Chen, Z. Wu, X. Ye, G. Guo, and Q. Qian, "The desaturation method of DMSP/OLS nighttime light data based on vector data: Taking the rapidly urbanized China as an example," *Int. J. Geograph. Inf. Sci.*, vol. 33, no. 3, pp. 431–453, 2019.

[29] F. Pozzi and C. Small, "Analysis of urban land cover and population density in the United States," *Photogrammetric Eng. Remote Sens.*, vol. 71, no. 6, pp. 719–726, 2005.

[30] C. Small, "Estimation of urban vegetation abundance by spectral mixture analysis," *Int. J. Remote Sens.*, vol. 22, no. 7, pp. 1305–1334, 2001.

[31] Q. Weng, D. Lu, and B. Liang, "Urban surface biophysical descriptors and land surface temperature variations," *Photogrammetric Eng. Remote Sens.*, vol. 72, no. 11, pp. 1275–1286, 2006.

[32] Q. Weng, D. Lu, and J. Schubring, "Estimation of land surface temperature-vegetation abundance relationship for urban heat island studies," *Remote Sens. Environ.*, vol. 89, no. 4, pp. 467–483, 2004.

[33] C. D. Elvidge *et al.*, "A fifteen year record of global natural gas flaring derived from satellite data," *Energies*, vol. 2, no. 3, pp. 595–622, 2009.

Xiaolei Huang is currently working toward the B.S. degree in geographic information science at the School of Geographical Sciences, Southwest University, Chongqing, China.

Her research interests include nighttime light remote sensing and urban geography.

Kaifang Shi received the Ph.D. degree in cartography and geographic information systems from East China Normal University, Shanghai, China, in 2017.

He is currently an Associate Professor with the School of Geographical Sciences, Southwest University, Chongqing, China. His research interests include remote sensing analysis in socioeconomic characterization and urbanization process, nighttime light remote sensing, and urban geography.

Yuanzheng Cui received the B.S. degree in geomatics engineering from Wuhan University, Wuhan, China, in 2011, and the Ph.D. degree in geography and resource management from the Chinese University of Hong Kong, Hong Kong, China, in 2016.

He is currently an Associate Professor with Zhejiang University of Finance and Economics. His research interests include remote sensing and geographic information system.

Yuanqing Li received the B.S. degree in chemistry, and M.S. degree in quaternary geology, in 2003 and 2010, respectively, from Southwest University, Chongqing, China, where he is currently working toward the Ph.D. degree at the School of Geographical Sciences.

His research interests include spatial and regional analysis and land use planning.